

Citation for published version:

Cuomo, S, Malfense Fierro, G-P & Meo, M 2022, Remote damage inspection with AR custom headset. in NG Meyendorf, NG Meyendorf, S Farhangdoust & C Niezrecki (eds), *SPIE SMART STRUCTURES + NONDESTRUCTIVE EVALUATION: NDE 4.0, Predictive Maintenance, and Communication and Energy Systems in a Globally Networked World*. vol. 12049, 1204906, Proceedings of SPIE - The International Society for Optical Engineering, vol. 12049, SPIE, NDE 4.0, Predictive Maintenance, and Communication and Energy Systems in a Globally Networked World 2022, Virtual, Online, 4/04/22. <https://doi.org/10.1117/12.2615290>

DOI:

[10.1117/12.2615290](https://doi.org/10.1117/12.2615290)

Publication date:

2022

Document Version

Peer reviewed version

[Link to publication](#)

University of Bath

Alternative formats

If you require this document in an alternative format, please contact:
openaccess@bath.ac.uk

General rights

Copyright and moral rights for the publications made accessible in the public portal are retained by the authors and/or other copyright owners and it is a condition of accessing publications that users recognise and abide by the legal requirements associated with these rights.

Take down policy

If you believe that this document breaches copyright please contact us providing details, and we will remove access to the work immediately and investigate your claim.

Remote damage inspection with AR custom headset

Stefano Cuomo^a, Gian Piero Malfense Fierro^a, Michele Meo^{*a}

^aDepartment of Mechanical Engineering, University of Bath, Bath, BA2 7AY, UK

*m.meo@bath.ac.uk;

ABSTRACT

Nowadays key factors in high technology industries are digitalization, networking, data management, informatization and automation. The mutual interactions between these factors led toward the quickly evolving industrial revolution called “Industry 4.0” (or IR4) defined as the integration of new technologies within the design, manufacturing, and maintenance processes. This dynamic scenario is made possible by the so-called Internet of Things (IoT). In this context the inspection sector is rapidly upgrading in order to cope with the new technology paradigm of industry. The application of new technologies in NDE can improve the effectiveness, in terms of time and costs, of many inspection processes and include much more data and details exploiting multiple devices and sensing systems (NDE 4.0). In this work a remote damage inspection device is introduced, based on a stereo-laser depth map system connected to a custom headset. A laser speckle pattern is projected on the inspected component and acquired through a stereo cameras system. Damage is detected as a change in the depth map. The detected damage is then superimposed on the structure and streamed to the headset. The proposed idea would be extremely beneficial during the inspection process of large structures to assess whether a damage is present. This, in turn, would make inspections and analysis faster with overall benefits in terms of cost efficiency and availability of the product.

Keywords: SHM, damage detection, remote inspection, remote NDE, BVID, industry 4.0, stereo vision, laser, headset, AR.

1. INTRODUCTION

In the last decade, developments in technology as digitalization, networks, data management, informatization and automation, induced the birth of ‘Industry 4.0’ (IR 4) which focuses on the nature of Human-machine interaction, in particular with new paradigms such as Internet of Things (IoT) and Cyber-Physical Systems (CPS) [1]. IoT is defined as a global infrastructure for the information society, enabling advanced services by interconnecting (physical and virtual) things based on existing and evolving interoperable information and communication technologies [2]. In other terms we can consider any device embedded with sensors, processors, software and able to communicate and transfer data with other systems via internet or any network as IoT. Industry 4.0 can be naturally considered as the Fourth Industrial Revolution and involves the integration of new technologies within the manufacturing process, and how these provide improvements in global efficiency. Main aspect of this novel paradigm is referred to as Smart Manufacturing, which can be described as the integration of sensors, communication technology, computing platforms, simulations, data modelling and predictive engineering within production manufacturing assets [3]. In this context the “health” inspection sector is quickly adapting and upgrading to cope with this new industrial environment. Deploying industry 4.0 key elements upon the non-destructive evaluation (NDE) and structural health monitoring (SHM) procedures and operations can lead to improvements in terms of time and costs of many inspection processes, hence be more effective exploiting multiple devices and sensing systems. The information from NDE is extremely valuable and in some cases vital for a system or product life, and industry 4.0 is making this flow of data even more important and relevant leading to a so called NDE 4.0. The latter can be defined as cyber-physical non-destructive evaluation, from the combination of IR4 digital technologies and physical inspection methods leading to enhanced inspection performance, quality, sustainability which in turn can improve design, production and maintenance [4], [5]. Important elements introduced in this smart environment are sensing, identification, control systems, and importantly machine vision systems. In this work a remote damage inspection device is introduced, based on

a stereo-laser depth map system connected to a custom headset. A laser speckle pattern is projected on the inspected surface and acquired through two high resolution cameras (stereo). Any damage is detected as a change in the depth map, generated through a routine specifically developed, evaluating specific extracted features from the acquired images. The damage information is then superimposed on the structure and streamed to the headset. Similar applications are present in literature, da Costa et al. used laser speckle projection with temporal correlation for improved 3D active stereo measurements for free form surfaces [6]; Cunha et al. developed a laser speckle acquisition system with stereo vision to observe skin surface and identified critical physiological states using a dissimilarity descriptor [7]; Stewart et al proposed a laser speckle perfusion imaging to evaluate burn scar perfusion and found that the method had higher resolution and faster scan time compared to the traditional methods [8]. The proposed idea would be extremely beneficial during the inspection process of large structures to assess whether a damage is present, indeed any operator or engineer could evaluate the state of components remotely without being in the maintenance facility. This, in turn, would make inspections and analysis faster with overall benefits in terms of cost efficiency and availability of the product. The proposed system is capable to detect and evaluate small damages/dents and highlight them in the custom headset with a stereo vision graphic, making it clear the entity of the detriment and then in case actuate the proper mitigation measures. A custom light weight stereo vision headset was designed and manufactured, with Ultra High-Definition and high refresh rate (120 Hz) monitor.

2. REMOTE DAMAGE DETECTION SYSTEM

As discussed in the introduction, the aim of this work was the development of a remote damage detection system. To achieve this target, the authors exploited the stereo vision technology using high resolution cameras to generate a depth map able to detect a damage or defect on any inspected specimen. Compared to previous systems and tools presented in literature the proposed solution exploits a speckle pattern projected with a laser to increase and enhance surfaces irregularities and thus the characteristic features to be extracted from the processed images, similarly applied for 3D sensing systems [9], [10]. Once generated, the depth map is examined to determine the presence or not of any damage or flaw of the observed area. Afterwards, the information related to an eventual damage are collected, and sent to the custom headset, where a real time image of the analyzed area is in streaming. An augmented reality scene is obtained adding digital elements to the live view of the specimen, embedding info about damage location and damage characteristics such as length and depth.

In the subsections below there is a brief discussion about the key elements of the system developed, the stereovision, augmented reality and the description of the custom headset specifically designed for this application.

2.1 Stereo Vision

In the last decade stereo vision (SV) systems became a major technique to acquire three-dimensional information from surrounding environment or from selected objects. Field of application are many and it is possible to mention object and people detection, autonomous vehicles to detect obstacles, robot control, industrial automation, space operations and medical [11]–[16]. SV works similarly to human 3D vision and is based on triangulating rays from many different viewpoints; indeed, using two cameras it is possible to retrieve depth information finding the corresponding points in two different images. Considering a system with two cameras having the same characteristics and focal distance, and image plane placed at certain distance, depicted in Figure 1.

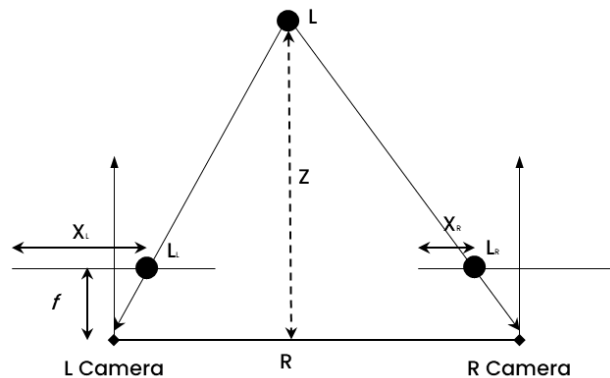


Figure1. Depth and disparity from triangulation.

An object located in L is observed at distances X_L and X_R from the left and right cameras respectively. The distance, considering similar triangles, is given by the following:

$$Z = \frac{R * f}{x_L - x_R} \quad (1)$$

Where f is the focal distance, and the difference $x_L - x_R$ is defined as the disparity of the point L and R is the reference distance between the two cameras. A fundamental step for any SV system is the calibration process, involving the alignment of pixel information between the two considered cameras in order to identify the 3D information for each pixel in the image and determine which pixels in different images match the same real object (correspondence problem). The latter is usually solved applying the epipolar constraint, that enables stereo correspondence on a straight line after rectification of the stereo images. With this constraint the search of matching region becomes a 1D problem [17][18]. The relation between the obtained disparity and depth is given by equation 1 above, and it is clear how disparity assumes higher values for points closer to the cameras and vice-versa, thus minimum values of the disparity map correspond to higher depth in the field of view.

2.2 Augmented reality (AR)

Augmented reality (AR) in the last years had a vast application in multiple and diverse fields such as gaming, education, retail, tourism, medical training and industry[19]–[22]. AR, generally enhances the perception of the real world by overlaying virtual objects on real images [21]. AR has been used within the Industry 4.0 paradigm in networks of connected physical systems and human-machine communication [23]. One of the main issues relating to AR in real-time systems, is the latency of the process pipeline, which includes the image capture from the sensor, image processing steps including object tracking/manipulation or avatar animation, and in terms of online systems, the server, network, and client latencies [24]–[26]. The principal industrial field of applications of AR are maintenance, automotive, aviation, consumer and nuclear. One of the industry sectors that has seen a considerable implementation of AR is within the repair and maintenance operations, providing the operators with useful information, suggesting tasks, and highlighting eventual errors. A specific application proposed was embedding AR and Active Infrared Thermography (IRT) which has resulted in improvements in the speed of maintenance operators, due to fewer mistakes and less cognitive loads [27], [28]. In this context, the application of AR technologies has an increasing trend as the IoT sector is fast growing, with more and more devices and network connected. For this reason, this work aim was the development of a system included in the IR4 paradigm, with a sensing system able to communicate in real time with a custom headset, to remotely stream vital information about the damage state of a structure, and direct the consequent actions needed to remove or mitigate the damage.

2.3 Developed Vision System and Custom Headset

The VS developed is composed by two 20 MP, grey-scale, USB cameras (Daheng Imaging MER-2000-19U3M) with high frame rate and 12-bit depth sensor along with two 12 mm focal length and 2.8F aperture lenses. A point laser (Laser Components FLEXPOINT) with 645 nm design wavelength was used to generate a random speckle pattern, with a specific DOE attached.

The algorithm developed for the execution of the damage estimation consisted of the calibration process, the stereo correspondence, rectification and depth map estimation. A specific routine was developed to acquire two frames, from both the cameras simultaneously, for the calibration step. A total of 20 images, ten for each camera, were acquired and then processed with the stereo camera calibrator routine included in MATLAB. The calibration was performed to acquire focal length, optical center, lenses distortion (defined as intrinsic parameters) and the location of the cameras, evaluating rotation and translation i.e., the rigid transformation from the real-world coordinate system to the cameras coordinate system (defined as extrinsic parameters) [29]–[32]. In Figure 2 below a frame of the calibration process, performed with a checkboard pattern. The evaluated stereo parameters were then stored to be used in the consequently routine for the depth map evaluation. The latter starts with local feature detection and extraction, that enables to evaluate sharp differences between image areas characterized by variations in color, intensity, and texture. This process helps the determination of correspondence between two images notwithstanding their eventual differences, such as rotation or changes in view. In this case we use the blob feature type implementing the Speed-Up Robust Feature algorithm (SURF) recommended for point correspondence and classification and moreover it is not affected by scale and rotation of the images [33]. This detector is based on the determinant of the Hessian matrix that ensures good level of accuracy; where the determinant

assumes maximum values blob shaped structures in the image are detected. The Hessian matrix of a point $\mathbf{x} = (x, y)$ in a given image I with a specific scale s , is given by the following [33]:

$$H(\mathbf{x}, s) = \begin{bmatrix} L_{xx}(\mathbf{x}, s) & L_{xy}(\mathbf{x}, s) \\ L_{xy}(\mathbf{x}, s) & L_{yy}(\mathbf{x}, s) \end{bmatrix} \quad (2)$$

where $L_{ij}(\mathbf{x}, s)$ is the Gaussian second order derivative $\frac{\partial^2}{\partial x^2} g(s)$ convoluted with the image I . Once the maxima of the determinant of the Hessian matrix are evaluated an interpolation is executed in image and scale space, and interest points are localized with blob structures [33].

This step is fundamental to perform the rectification of the left and right images acquired with the cameras, indeed after the feature extraction the corresponding points are found, matching the two images' descriptors, then the outlier matching points are removed imposing the epipolar constraint, and finally the rectification is performed.

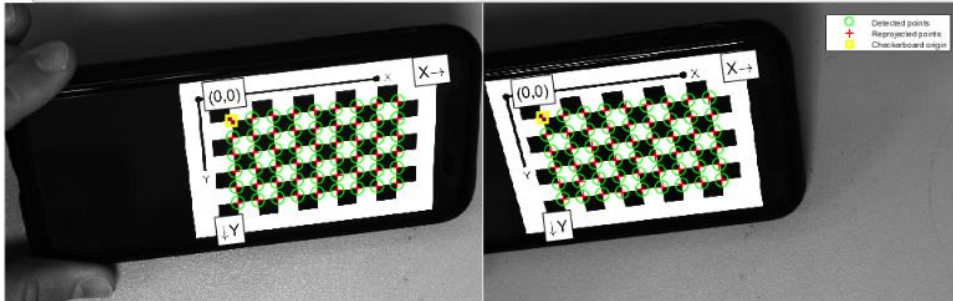


Figure2. Calibration process with checkboard pattern.

Finally, the disparity is evaluated and thus the depth map of the image can be determined, considering the relation between depth and disparity described in Equation1. A schematic representation of the algorithm developed is in Figure 3.

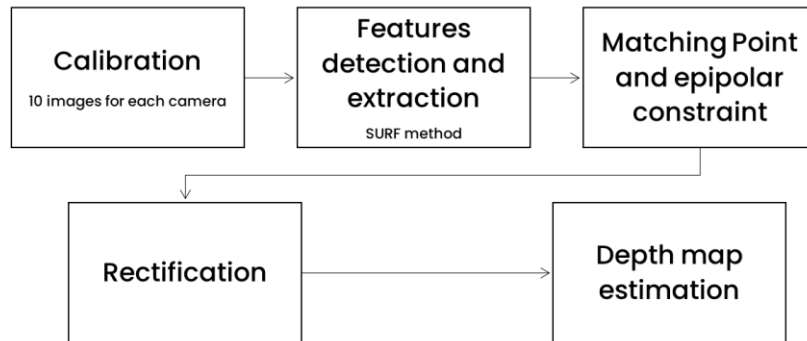


Figure.3 Block scheme of the developed algorithm.

The custom headset built for this application was specifically designed to have lightweight, high comfort, flexible adjustments, simultaneous screen and real-world views, high resolution, and high refresh rate screen. Hence, a custom design was finally selected and then manufactured with stereolithographic resin printer, ensuring a weight under 500 grams for the full headset. Pupil distance of the lenses and screen distance are controlled with rollers fitted on the headset body ensuring adjustments for any user. A 2K resolution, 120 Hz refresh rate screen was embedded in the headset, ensuring low latency and high-quality streamed image.

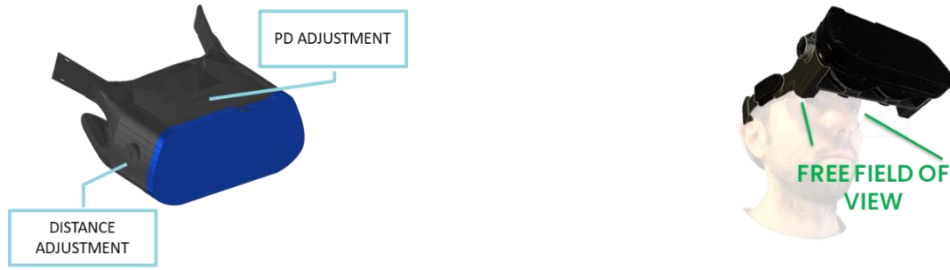


Figure 4. Custom headset (left) and field of view of the user (right).

3. EXPERIMENTAL SETUP

The setup to perform the damage estimation and streaming to the custom headset is reported in Figure 5, with details of the equipment and fixtures used.

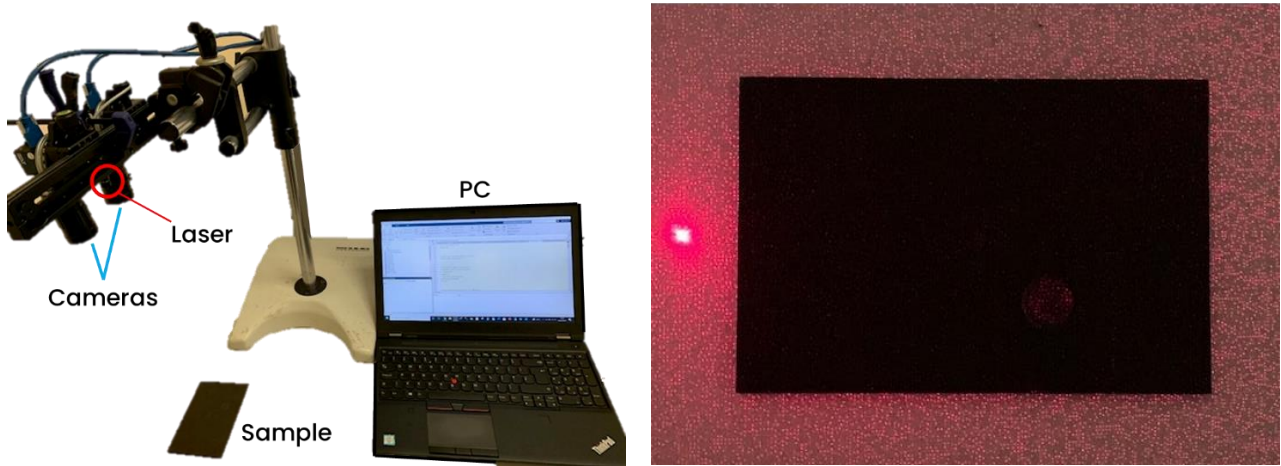


Figure 5. Experimental setup (left) and detail of the random speckle pattern projected (right).

From the figure above it is possible to observe the random speckle pattern, with 30000 distributed points, projected on the inspected samples; this projection enhances the local differences in the images leading to stronger features to be extracted for the correspondence step using the SURF method.

A total of five different samples were inspected with the proposed system, made of different materials and having different typology of surface damage or flaw. The first samples tested was a steel sample with a slot along the major dimension and half thickness deep. The second sample was a carbon fiber sample with a thermoplastic polyurethane coating impacted at low velocity impact, hence affected by an indent of the top surface. The third sample was standard carbon fiber sample, impacted with top surface indentation and lower surface full fracture. The fourth sample was an aluminum block with four circular slots on the top surface, each of them having different depth (2,2.5,3,4 mm respectively) Table 1 reports all the samples considered for the experimental campaign and the characteristics of each damage examined.

	<ul style="list-style-type: none"> • Sample dimensions: 124 mm x 40 mm x 12mm • Damage: 124 mm x 0.5 mm x 4.5 mm
--	--

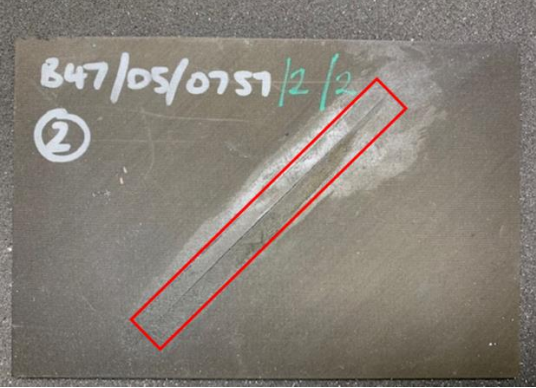
	<ul style="list-style-type: none"> • Sample dimensions: 150 mm x 100 mm x 12 mm • Indentation: 7 mm x 0.1 mm
	<ul style="list-style-type: none"> • Sample dimensions: 150 mm x 100 mm x 5 mm • Indentation: 8 mm x 0.5 mm • Lower fracture: 95 mm x 15 mm x 1 mm
	
	<ul style="list-style-type: none"> • Sample dimensions: 150 mm x 89 mm x 11 mm • 4 circular slots: Ø 12mm x 2-4 mm depth

Table 1. Samples examined and characteristic dimension.

4. RESULTS

In this section all the results of the damage detection using stereo depth map are listed, with discussion for each examined sample, highlighting the effectiveness of the method to evaluate the presence of any flaw on the surface inspected.

4.1 Steel Sample

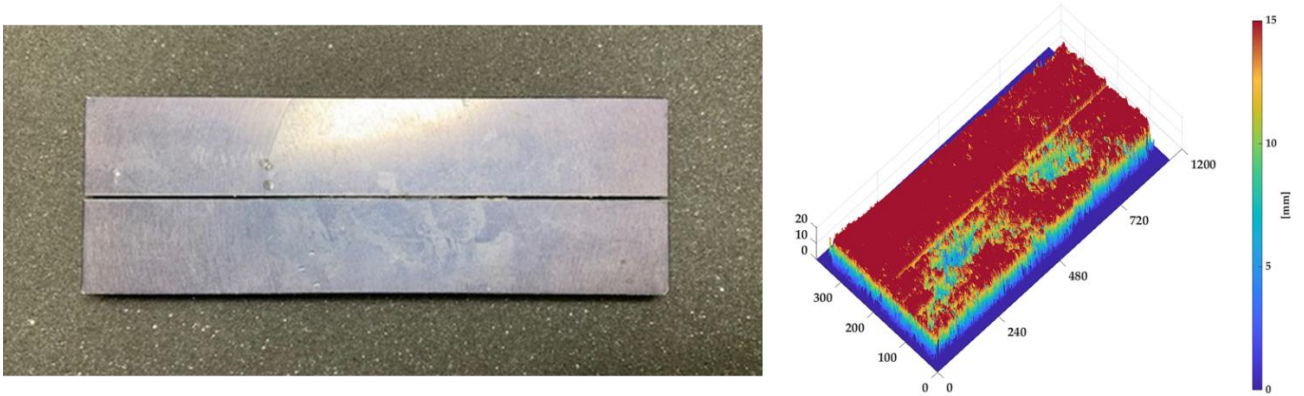


Figure 6. Depth map of the steel sample.

Figure 6 shows the depth map of the steel sample analyzed with the proposed method. It is possible to appreciate the good estimation of the dimensions of the damage and its depth, with representation in 3D perspective. The central slot is clearly detectable from the 3D depth map, standing out from the rest of the sample, consistent with its real dimension of 5 mm.

4.2 TPU Coated CFRP sample

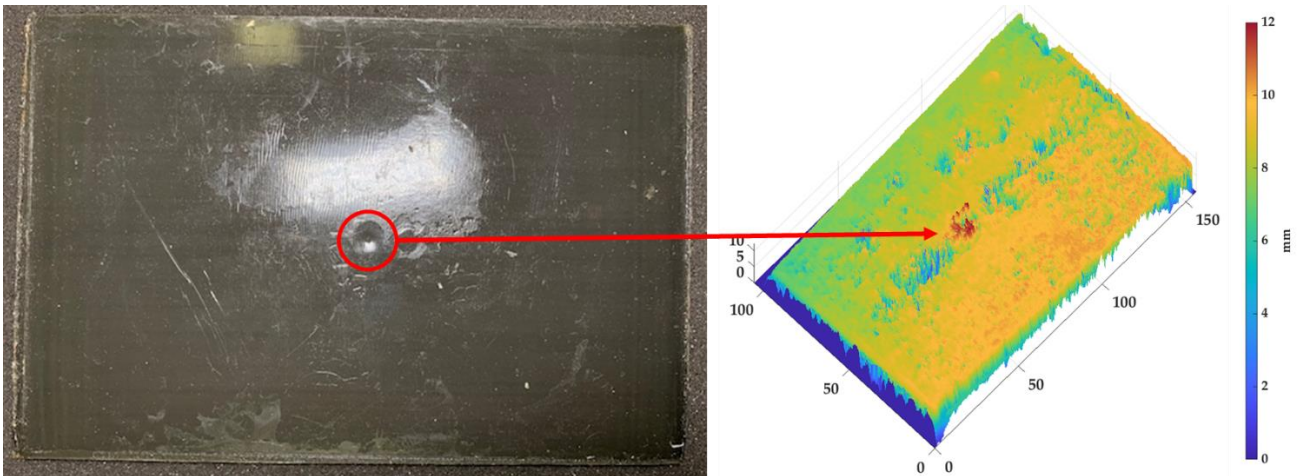


Figure 7. Depth map of the TPU coated sample.

In Figure 7 the 3D depth map for the TPU coated sample. It is interesting to observe the clear indentation on the depth map, (circled in red) corresponding to the indentation on the sample (red arrow). The system recognizes it as a bump rather than a depression on the surface of the sample, indeed the depth map assumes the maximum value rather than an intermediate decreased value, as expected. This might be due to scattering and reflection issue of the speckle pattern. Nevertheless, the system was able to recognize as specific area that was not uniform compared to the pristine sample, and this is relevant considering that the indent is only 0.1 mm.

4.3 CFRP sample

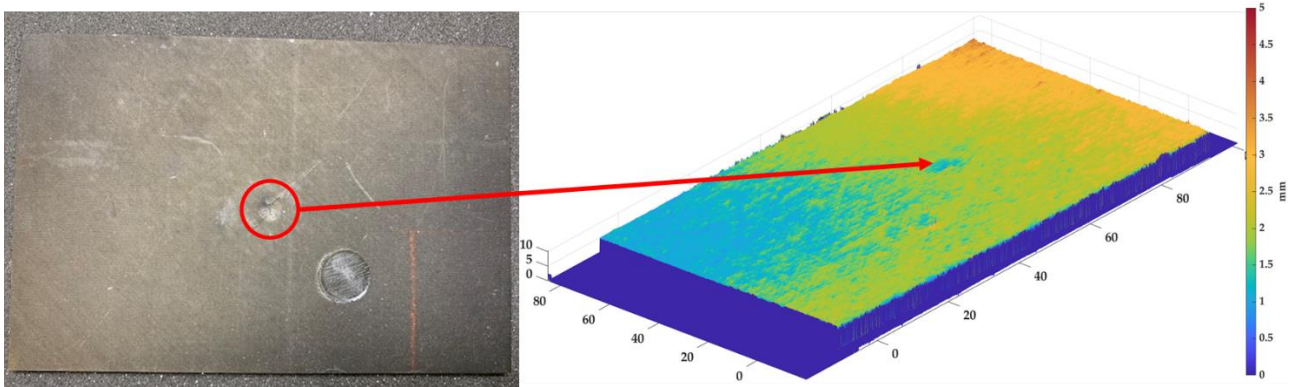


Figure 8. Depth map of the CFRP sample.

Result from the standard CFRP sample, Figure 8, shows good estimation of the indentation (red circle) caused by the impact, with an error around 0.5 mm respect the depth of the indentation measured on the sample (0.2 mm). In this case, being the surface not so reflective compared to the TPU sample, the results are considerably more precise. The 3D representation effectively represents the damage induced on the sample.

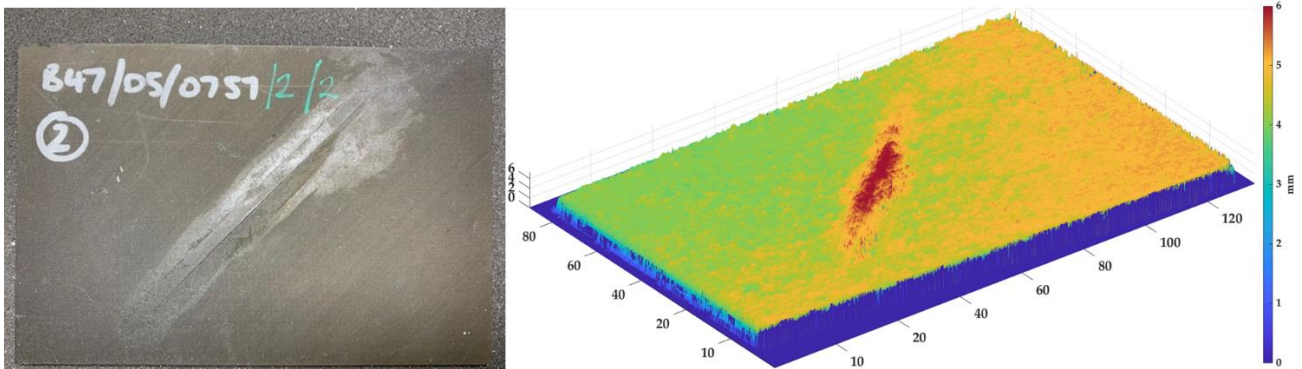


Figure 9. Depth map of the CFRP sample.

In Figure 9 the damage estimation from the lower surface of the same specimen considered above. In this case the damage is an evident fracture, with layers directed out of plane. The peak due to the damage measured on the sample was around 1 mm, and this is in good agreement with the measure gathered with the proposed method (~1mm). Even in this case, the surface quality is not affecting the acquisition through the cameras, with outstanding result in terms of measured damage, and quality of the three-dimensional image.

4.4 Aluminum sample

The aluminum sample with four circular slots presented a surface quite reflective, nevertheless the proposed method was able to properly detect the depression on the inspected sample with precision consistent with the previous results.

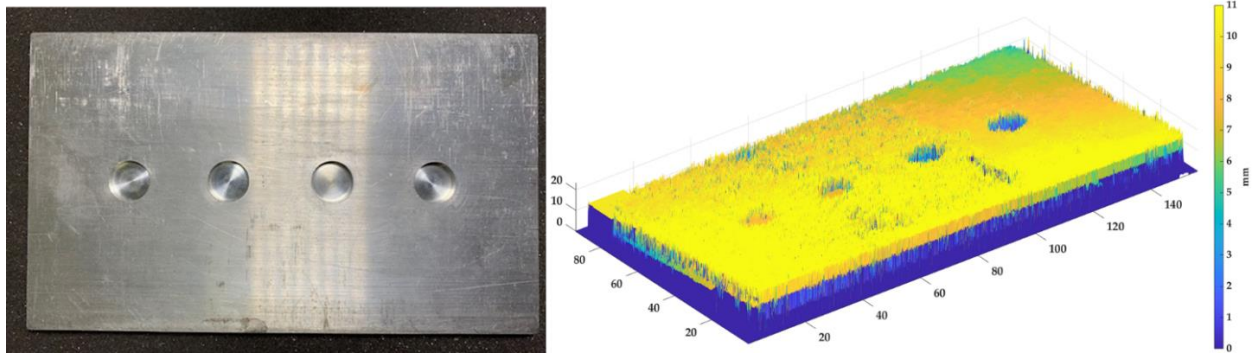


Figure 10. Depth map of the aluminum sample.

In this case to have a clear visualization of the damage the scale needed to be extended beyond the sample maximum thickness. As the depth map among the sample is not uniform, a problem with the rectification step probably occurred, mainly due to the reflective nature of the aluminum sample. In any case a good estimation of the damage dimensions and location was obtained with the proposed method, moreover, being able to detect the depth difference of the circular slots, considering that the maximum difference in depth is 2 mm.



Figure 11. Streaming of the depth map in real time to the custom headset.

All the depth map obtained were streamed in real time, to be visualized in the custom headset designed. The data streamed are affected by low delay, thus any damage detection can be effectively observed remotely, without the necessity to be present in the testing facility.

5. CONCLUSIONS

In this work a remote damage inspection device was introduced, based on a stereo-laser depth map system connected to a custom headset. A laser speckle pattern was projected on the inspected specimens and acquired through a stereo cameras system. Any damage was detected as a change in the depth map. The detected damage then was superimposed on the structure and streamed to the headset. Good results from the experimental campaign demonstrated the validity of the system, capable to detect damage with very good level of accuracy even for barely visible surface flaws or indents (below 1 mm depth). The proposed idea would be extremely beneficial during the inspection process of large structures to assess whether a damage is present, moreover being a cost-effective solution using non-expensive equipment and extensive software programming. This, in turn, would make inspections and analysis faster with overall benefits in terms of cost efficiency and availability of the product. The proposed system was capable to detect and evaluate small damages and highlight them in the custom headset with a stereo vision graphic, making it clear the entity of the detriment, vital information to actuate the proper mitigation measures to avoid any catastrophic event during the life cycle of main structures and components.

ACKNOWLEDGMENTS

The authors would mention Marco Boccaccio for the time spent, the support and help during the manufacturing of the custom headset.

REFERENCES

- [1] M. D. Di Nardo, D. Forino, and T. Murino, "The evolution of man-machine interaction: the role of human in Industry 4.0 paradigm," *Prod. Manuf. Res.*, 2020.
- [2] M. Gunturi, H. D. Kotha, and M. Srinivasa Reddy, "An overview of internet of things," *J. Adv. Res. Dyn. Control Syst.*, vol. 10, no. 9, pp. 659–665, 2018.
- [3] A. Kusiak, "Smart manufacturing," *Int. J. Prod. Res.*, 2018.
- [4] J. Vrana and R. Singh, "NDE 4.0—A Design Thinking Perspective," *J. Nondestruct. Eval.*, vol. 40, no. 1, pp. 1–24, 2021.
- [5] N. Riess and R. Link, "NDT 4.0 — Significance and Implications to NDT: Automated Magnetic Particle Testing as an Example," *NDT World*, 2019.
- [6] A. A. G. Jr and T. L. F. da C. Pinto, "3D Active Stereo Measurement in a Regular Mesh," vol. 6, no. c, pp. 281–289, 2014.
- [7] F. Cunha, L. Távora, P. Assunção, S. Faria, and R. FonsecaPinto, "Stereo laser speckle dissimilarity analysis using self-organizing maps," in *IFMBE Proceedings*, 2020.
- [8] C. J. Stewart, R. Frank, K. R. Forrester, J. Tulip, R. Lindsay, and R. C. Bray, "A comparison of two laser-based methods for determination of burn scar perfusion: Laser Doppler versus laser speckle imaging," *Burns*, 2005.
- [9] J. García, Z. Zalevsky, P. Garcia-Martinez, C. Ferreira, M. Teicher, and Y. Beiderman, "Projection of speckle patterns for 3D sensing," *J. Phys. Conf. Ser.*, 2008.
- [10] K. Fu, Y. Xie, H. Jing, and J. Zhu, "Fast spatial-temporal stereo matching for 3D face reconstruction under speckle pattern projection," *Image Vis. Comput.*, 2019.
- [11] J. J. Aguilar, F. Torres, and M. A. Lope, "Stereo vision for 3D measurement: Accuracy analysis, calibration and industrial applications," *Meas. J. Int. Meas. Confed.*, 1996.
- [12] A. El Gendy, A. Shalaby, M. Saleh, and G. W. Flintsch, "Stereo-vision applications to reconstruct the 3D texture of pavement surface," *Int. J. Pavement Eng.*, 2011.
- [13] L. Nalpantidis and A. Gasteratos, "Stereo vision for robotic applications in the presence of non-ideal lighting conditions," *Image Vis. Comput.*, 2010.
- [14] A. Broggi, M. Bertozzi, and A. Fascioli, "Self-calibration of a stereo vision system for automotive applications," *Proc. - IEEE Int. Conf. Robot. Autom.*, 2001.
- [15] K. W. Nam, J. Park, I. Y. Kim, and K. G. Kim, "Application of stereo-imaging technology to medical field," *Healthcare Informatics Research*. 2012.
- [16] N. Dalal and B. Triggs, "Histograms of oriented gradients for human detection," in *Proceedings - 2005 IEEE Computer Society Conference on Computer Vision and Pattern Recognition, CVPR 2005*, 2005.
- [17] S. Mattoccia, "Stereo vision algorithms for FPGAs," in *IEEE Computer Society Conference on Computer Vision and Pattern Recognition Workshops*, 2013.
- [18] A. Valsaraj, A. Barik, P. V. Vishak, and K. M. Midhun, "Stereo Vision System Implemented on FPGA," *Procedia Technol.*, 2016.

- [19] P. Sarkar, J. S. Pillai, and A. Gupta, "Scholar: A collaborative learning experience for rural schools using augmented reality application," in *Proceedings - IEEE 9th International Conference on Technology for Education, T4E 2018*, 2018.
- [20] M. Eckert, J. S. Volmerg, and C. M. Friedrich, "Augmented reality in medicine: Systematic and bibliographic review," *JMIR mHealth and uHealth*. 2019.
- [21] Z. Makhataeva and H. A. Varol, "Augmented reality for robotics: A review," *Robotics*. 2020.
- [22] R. Palmarini, J. A. Erkoyuncu, R. Roy, and H. Torabmostaedi, "A systematic review of augmented reality applications in maintenance," *Robotics and Computer-Integrated Manufacturing*. 2018.
- [23] D. Gorecky, M. Schmitt, M. Loskyll, and D. Zühlke, "Human-machine-interaction in the industry 4.0 era," in *Proceedings - 2014 12th IEEE International Conference on Industrial Informatics, INDIN 2014*, 2014.
- [24] R. T. Azuma, "A Survey of Augmented Reality, Presence: Teleoperators and Virtual Environments," *Found. Trends Human-Computer Interact.*, 1997.
- [25] R. Azuma, Y. Baillet, R. Behringer, S. Feiner, S. Julier, and B. MacIntyre, "Recent advances in augmented reality," *IEEE Comput. Graph. Appl.*, 2001.
- [26] G. Welch and E. Foxlin, "Motion tracking: No silver bullet, but a respectable arsenal," *IEEE Comput. Graph. Appl.*, 2002.
- [27] F. Lamberti, F. Manuri, A. Sanna, G. Paravati, P. Pezzolla, and P. Montuschi, "Challenges, opportunities, and future trends of emerging techniques for augmented reality-based maintenance," *IEEE Trans. Emerg. Top. Comput.*, 2014.
- [28] M. Ortega, E. Ivorra, A. Juan, P. Venegas, J. Martínez, and M. Alcañiz, "Mantra: An effective system based on augmented reality and infrared thermography for industrial maintenance," *Appl. Sci.*, 2021.
- [29] Z. Zhang, "A flexible new technique for camera calibration," *IEEE Trans. Pattern Anal. Mach. Intell.*, 2000.
- [30] J. Heikkila and O. Silven, "Four-step camera calibration procedure with implicit image correction," in *Proceedings of the IEEE Computer Society Conference on Computer Vision and Pattern Recognition*, 1997.
- [31] J.-Y. Bouguet, "Camera calibration toolbox for matlab: www.vision.caltech.edu/bouguetj/calib-doc," *Online documentation*, 2003. .
- [32] G. R. Bradski and A. Kaehler, *Learning OpenCV - computer vision with the OpenCV library: software that sees*. 2008.
- [33] H. Bay, T. Tuytelaars, and L. Van Gool, "SURF: Speeded up robust features," in *Lecture Notes in Computer Science (including subseries Lecture Notes in Artificial Intelligence and Lecture Notes in Bioinformatics)*, 2006.